Journal of Environmental Science Studies; Vol. 6, No. 2, 2023
ISSN 2591-779X E-ISSN 2630-4821
Published by July Press

Experimental Investigation on Velocity Fields of Seepage Flow Inside Gravel Mount

Youichi Yasuda[1] & Megumi Uemura[2]

[1] Department of Civil Engineering, College of Science and Technology, Nihon University, Tokyo, Japan

[2] Department of Civil Engineering, Graduate School of Science and Technology, Nihon University, Tokyo, Japan

Correspondence: Prof. Youichi Yasuda, Civil Engineering Dept., College of Sci. and Tech., Nihon University, Tower Schola S1010, 1-8-14 Kanda Surugadai, Chiyoda-ku, 101-8308 Tokyo. E-mail: yasuda.youichi@nihon-u.ac.jp

Received: July 15, 2023 Accepted: August 10, 2023 Online Published: September 17, 2023

doi:10.20849/jess.v6i2.1373 URL: https://doi.org/10.20849/jess.v6i2.1373

Abstract

There is little information on velocity field of seepage flows. The formation of seepage flow is significant for aquatic habitat including spawning of aquatic animals in river. To create spawning fields in river, the stability of a heaped-up gravels during floods is required for its artificial formation. The velocity measurement of seepage flows is also necessary. This paper presents velocity fields of seepage flows in a heaped-up gravels. The experimental study yields that the heaped-up gravels are stabilized by installing the consecutively assembled boulders on the gravels. Also, small mean velocity and standard deviation are recorded for different discharges. Spectrum analysis reveals that fluctuation velocity of seepage flows depends on the turbulent flow above the heaped-up gravels.

Keywords: seepage flow, gravel mount, assembled boulders, spawning bed

1. Introduction

The population of Ayu sweetfish (Plecoglossus altivelis), an amphidromous fish native to East Asia, has been reducing in Japan in recent years (Kono et al., 2017). One of the primary factors of this phenomenon is speculated to be river diversion, dam construction, and many other river regulation projects, causing the degradation and reduction of spawning habitat. Similar concerns are being raised in North America and Europe, where the decline of spawning habitat of salmonids is also a pressing issue (Wheaton and Pasternack, 2004). Spawning habitats in natural river are commonly formed where the tributary joins the main channel or at meandering river (where the velocity is relatively slow). Also, seepage flow within the gravel bed plays a crucial role in the spawning habitat as it provides fresh water to the spawn eggs and regulate the water temperature around them. There are numerous attempts to artificially construct spawning beds: gravel augmentation in riverbed (McManamay et al., 2010). McManamay introduced a mountain-like structure consisting of gravel as an ideal spawning model, while also highlighting the importance of a pool-riffle sequence in the spawning habitat. In Japan, as a fisheries project, attempts have been made to respond to the spawning season by provisionally laying gravels and cobble stones that can be used as spawning beds, but in many cases, when the spawning season coincides with a flooding event, the gravel is swept away, and the spawning environment is lost. Therefore, the stability of such an artificially constructed spawning bed is of an urgent demand. Also, clarifying the mechanism of seepage flow within gravel is beneficial for constructing a spawning-friendly riverbed. Despite the importance of elucidating seepage flow, its mechanism has rarely been examined. Previously, various approaches were taken to investigate the flow characteristics of seepage flow: tracing ‘dye’ within the riverbed by standpipes (Orchard, 1988), injecting artificial saline tracers underground to investigate the velocity of groundwater velocities (Schirmer et al., 2013). Additionally, Chanson and Zhuang (2015) measured the seepage bubbly flow in the cavity of a gabion stepped spillway weir by phase detection probe to determine the flow characteristics inside the gabion. Nevertheless, it is difficult to determine the actual velocity of seepage flow, as the subsurface flow is intricate and the apparatus to measure the velocity underground is not completely established.

The authors found that installation of enamel-coated metal coils inside gravel bed may be possible to measure

horizontal component of velocity of seepage flows by inserting a prove of electrical-magnetic current meter in the coil. This paper presents the velocity fields of seepage flows within a gravel heap beneath assembled boulders. The installation of assembled boulders may help the stability of gravels for a large discharge. To obtain different gradients of water surface at the same position, experiments were conducted under two different discharges. The velocity fields of seepage flows were investigated through mean velocity profile, standard deviation, change of velocity with time series, and spectrum analysis. The experimental results reveals that the seepage flow with low velocity including turbulence is always formed inside the heaped-up gravels, and the indirect assessment of the seepage flow based on water surface gradient and riverbed material may be limited under the set experimental condition.

2. Experimental Methods

2.1 Experimental Model

The experiment was conducted in a 17 m long, 0.40 m wide, 0.60 m deep slope-changeable rectangular channel which was set in a horizontal state. The experimental model is shown in Photo 1. Gravel with an average grain diameter of 0.016 m (based on the averaged value of long length, short length, and thickness) was stacked 5.5m downstream of the sluice gate, which is located at the center of the channel, for a length of 3.2 m. The stacked gravel was heaped into a mountain like shape (hereafter referred to as *gravel mount*), having its peak at 1m from the upstream edge of the model. The upstream slopes of the gravel mount are adjusted as 12 % averaged gradient (0.12 m height and 1.0 m long), while the downstream slope is adjusted as 5.5 % averaged gradient (0.12 m height and 2.2 m long). To prevent the gravels from being transported downstream, sharp-edged boulders (with an average grain diameter of 0.15m) that have been assembled to maintain its stability were installed on top of the gravel for a distance of 1.14 m, starting 0.30 m downstream from the upstream edge of the model: 0.70 m long at the adverse slope region, and 0.44 m long at downward slope region. Further, cobble stones (with an average grain diameter of 0.04 m) were installed on top of the gravel for a distance of 0.65 m, further downstream, to resemble a spawning bed.

(a) Gravel mount (heaped-up gravels)

(b) Upstream part of the experimental (sharp-edged boulder installation area)

(c) Downstream part of the model (cobble stone installation area)

Photo 1. Experimental model

2.2 Measurement Instrumentation

To measure the velocity of seepage flow inside the gravel mount, a total of nine coils with an inner diameter of 0.02 m and a spacing of 0.01 m was embedded inside the gravel mount with the end of the coil reaching the channel bed (Photo 2 (a)). Each coil was thoroughly enamel-coated to avoid interference with the magnetic field generated by the probe of the velocity meter. Aluminum cylindrical rods filled with cement concrete shown in Photo 2 (b) were inserted into each coil to prevent the gravel from entering the coil during non-measurement. This experiment was conducted under prototype conditions because no studies have directly evaluated seepage flow inside the gravels. Two different discharges were presented to investigate the effect of water surface gradient on the velocity fields inside the gravel mount: 0.0174 m^3/s (with a critical depth of 0.06578 m) and 0.0451 m^3/s (with a critical depth of 0.109 m). Water depth and bed morphology were measured using a point gauge. For velocity measurements, an I-type probe electrical-magnetic current meter KENEK CO. model VM-806H/VMT2-200-04P, sampling frequency 20 Hz and measurement time 30s for a total of 601 point-values measurements was used (Beretta and Yasuda 2023). To measure the velocity inside the gravel mount, the probe of the velocity meter was positioned at the center of the coil, and the velocity measurements were taken starting from the channel bed. Measurements are taken along the x, y, and z axes. The x-axis represents the longitudinal component, the y-axis represents the cross-sectional component, and the z-axis represents the vertical component. The x-axis originates 5.5 m downstream of the sluice gate, the y-axis at the channel center, and the z-axis at the channel bed.

(a) The enamel-coated coils with the cylindrical rods inserted

(b) Measurement points

Photo 2. Velocity measurement using coils and cylindrical rods

3. Results

3.1 Description of Flow Condition

Photo 3 shows the flow passing over the gravel mount. When the flow passes over the peak of gravel mount, it undergoes a transition from subcritical flow to supercritical flow, and then gradually transitions back to subcritical flow in the downstream. The water surface shows no significant waves being formed, although a slight change in surface flow is observed in the downstream part of the model. This flow condition can be attributed to local flow created at the downstream part of the model. The local flow is created when the main flow — where the maximum velocity is recorded at each measured cross section — is located near the water surface (referred to as a surface jet flow). The water level downstream is adjusted as the lowest water level required to form a surface jet flow. No sediment transport was observed at the downstream part of the model resembling spawning bed.

(a) Case 1: Q = 0.0174 m^3/s

(b) Case 2: Q = 0.0451 m^3/s

Photo 3. Flow conditions passing over the gravel mount

3.2 Gravel Bed Profiles and Water Surface Profiles

Figure 1 shows the ground profiles and water surface profiles at the center of the channel for Case 1 and Case 2. Blue and orange lines show the water surface profiles, black solid line shows the ground profile (in the installation region of assembled boulders and cobble stones, the top of the boulders and stones is corresponded) and gray broken line shows the profile of the gravel mount. As the water discharge increases, the overall water level rises on both supercritical flow region and subcritical flow region. Plus, the water surface profile indicates a surface jet flow with slight surface irregularities at the downstream of local flow. Figure 2 shows the estimated water surface gradient at the intervals of 0.20 m for Case 1 and Case 2. At the near peak of the gravel mount, where the transitioning to subcritical flow to supercritical flow take place at $x < 2.40$ m, the local maximum value of water surface gradient is approximately located at $x = 1.70$ m in both cases. In Case2, the second maximum value occurs approximately at $x = 0.75$ m, owing to the increase of water discharge which results in the rise of water level behind the gravel mount. At $x \geqq 2.40$ m, the value of the water surface gradient varies considerably due to the formation of surface jet flow.

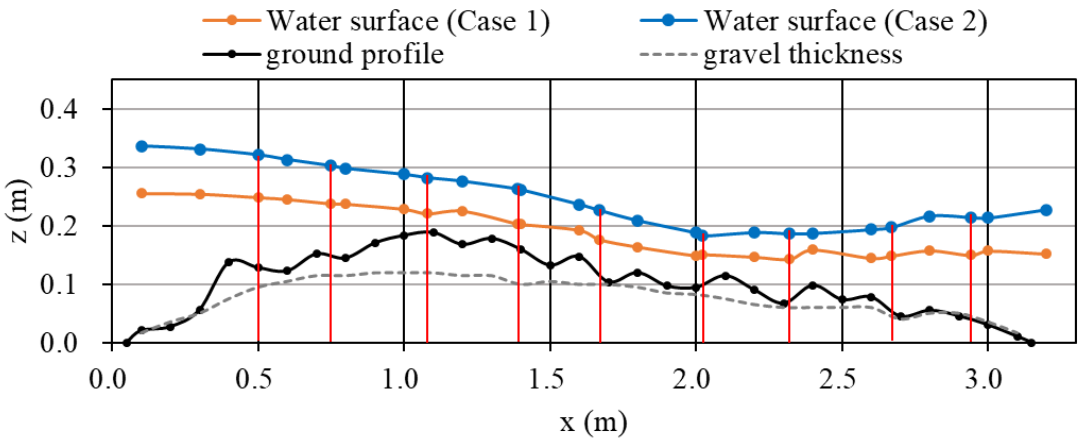

Figure 1. Water surface and ground profiles at the center of the channel

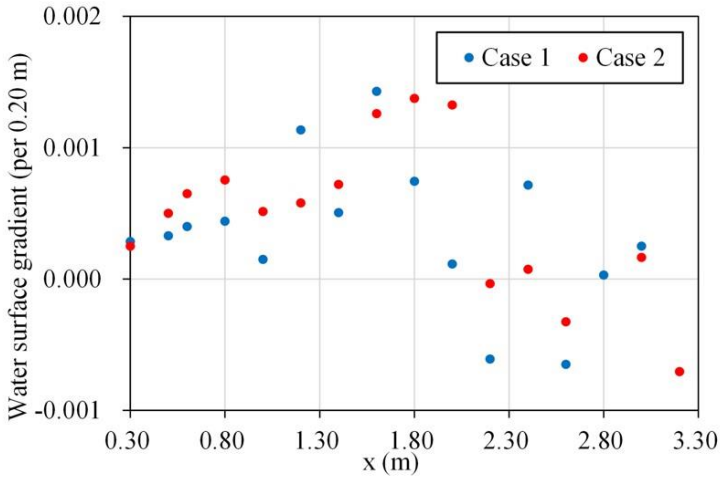

Figure 2. Water surface gradient at intervals of 0.20 m for Case 1 and Case 2

3.3 Velocity Profiles

Figure 3 shows the vertical distributions of mean velocity and standard deviation for x and y components at the center of the channel. Here the blue and orange lines show the mean velocity for x and y directional components, respectively. The gray and yellow lines show the standard deviations for x and y directional components, respectively. The shown velocity profiles include the velocity outside and outside of the gravel mount. As shown in this figure, the mean velocity inside the gravel mount is kept under 0.10 m/s, and the disturbance (as indicated by the standard deviation) is kept under 0.02 m/s. The mean velocity and disturbance inside the gravel mount are maintained at extremely low levels, owing to the random and intricate nature of the stacked gravel which restricts the speed of the flow. These velocity properties are consistently observed among the measured location, including the sharp-edged boulder installation area, cobble stone installation area, and downstream section where the gravels are exposed. However, at x = 0.50 m where the flow enters the gravel mount, and at x = 2.94 m where the gravel is relatively less thick, the velocity characteristics are easily influenced by the surrounding flow condition, although the mean velocity and disturbance are kept small.

By comparing the data collected at x = 0.75 m and x = 1.67 m, which cross-sections are located at the sharp-edged boulder installation area where the water surface slope is relatively large, no significant difference is observed in the mean velocity and disturbance inside the gravel mount. However, upon further inspection on the flow characteristics near the gravel mount, it reveals that the disturbance in the downstream cross-section (data at x = 1.67 m) is larger compared to that in the upstream cross-section (data at x = 0.75 m). This phenomenon can be attributed to a development of boundary layer generated when the flow passes over the peak of the gravel mount: at the upstream cross-section, the boundary layer is in the process of developing, while at the downstream cross-section, the boundary layer has fully developed (Ohtsu and Yasuda, 1994).

At x = 2.32 m, where the cobble stones are installed, the velocity characteristics among the cobble stones (0.05 < z (m) < 0.08) are influenced by the surface flow (z > 0.08 m) over the boulders. Nevertheless, the velocity inside the gravel mount remains small, similar to that upstream.

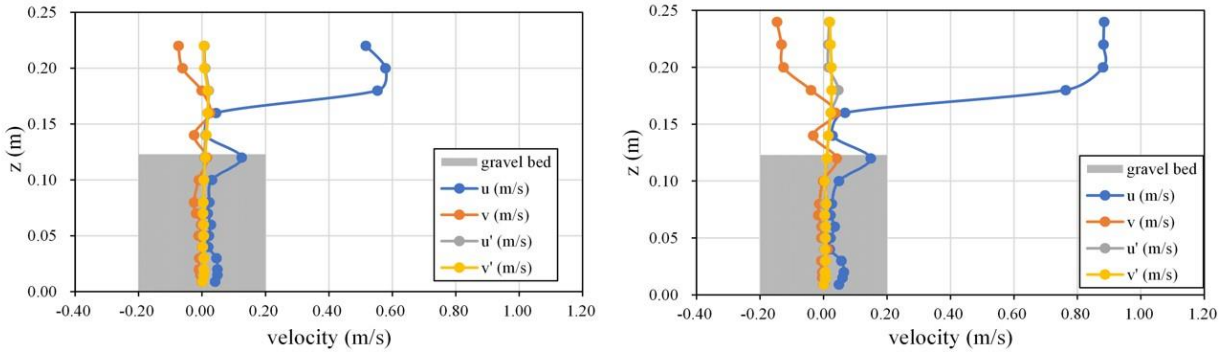

(a) Velocity distribution at x = 0.75 m for Case 1 (left) and Case 2 (right)

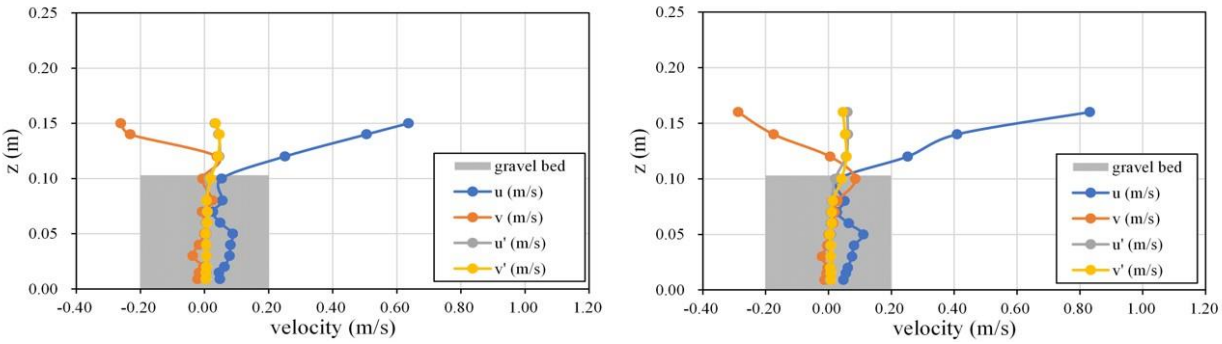

(b) Velocity distribution at x = 1.67 m for Case 1 (left) and Case 2 (right)

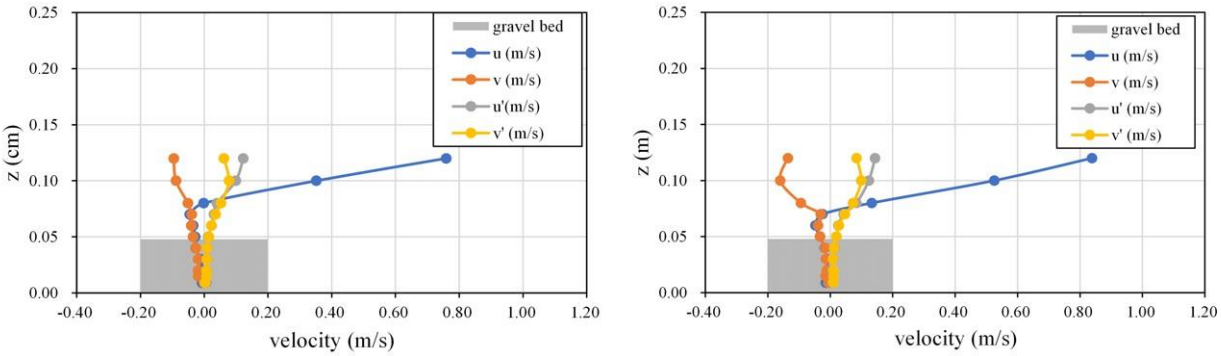

(c) Velocity distribution at x = 2.32 m for Case 1 (left) and Case 2 (right)

Figure 3. Velocity Distributions for Case 1 and Case 2

3.4 Velocity Properties of Seepage Flow

Figure 4 shows the longitudinal variation of the averaged flow velocity inside the gravel mount (the vertical cross-sectional average of the time-averaged velocity of the seepage flow in each measured section, defined as u_{ave}). In comparison with the Figure 2, similar pattern can be identified in the Figure4, and the correlation between the water surface gradient and the averaged velocity of seepage flow can be deduced. At 0.50 < x (m) < 2.50 (at the downstream part of the model), local maximal value of averaged velocity of seepage flow takes place at approximately x = 1.50 m. This indicates that the velocity of seepage flow is high in areas where the water surface slope is steep. It was observed in the Figure 4 that the second local maximal value of the water surface gradient occurs approximately at x = 0.75 m; however, averaged velocity of seepage flow did not exhibit the same trend. Nevertheless, from an overall view, it can be said that local maximal value of the water surface slope occurs approximately at x = 1.50 m, corresponding to that of the average velocity of seepage flow.

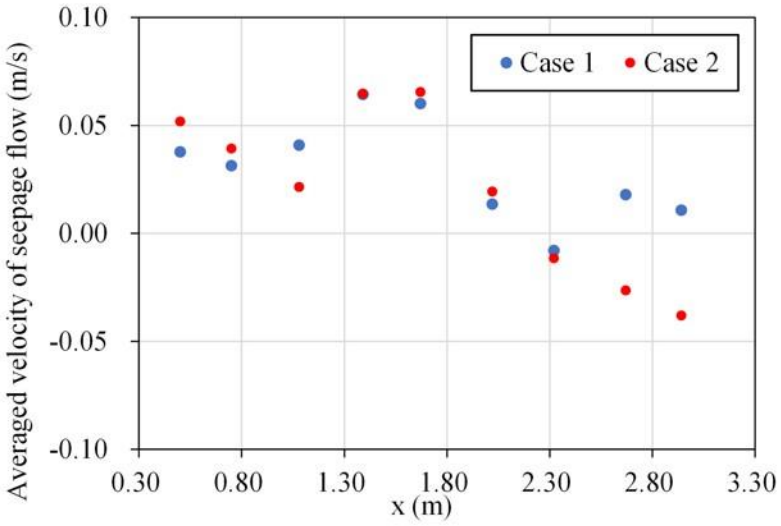

Figure 4. Longitudinal variation of the averaged flow velocity inside the gravel mount

3.5 Time Series of Longitudinal Component of Velocity

Figure 5 shows the time-series of longitudinal velocity for Case 2, including the data of the outer flow region and inner flow region, respectively. Based on the graph that depicts the time-series of velocity of the inner flow region (Figure 5(a)), constant fluctuations can be observed, although the deviations remain small. Furthermore, as the deviations of the velocity in the outer flow region becomes larger, the deviation of the inner flow region increases correspondingly.

At x = 0.75 m, where the boundary layer generated when the flow passes over the peak of the gravel mount is still growing, minor deviations are observed outside the newly boundary layer generated at z = 0.20 m, 0.22 m, and 0.24 m as shown in Figure 5 (a). While intermittent occurrences of low velocity are observed at z = 0.18 m since it is located directly beneath the boundary layer (Ohtsu and Yasuda, 1994). As for the seepage flow (inner flow region), the mean velocity remains consistently small with deviations smaller than those observed outside the boundary layer, near the water surface.

At x = 1.67 m, the measurements were taken inside the boundary layer as time-series data. Compared with the data on the upstream (x = 0.75 m), the deviations of the mean velocity at the surface of the model are larger at x = 1.67 m. In addition, at the inner flow region (Figure 5 (b)), the deviation is large near the surface of gravel mount. These characteristics are due to the unreduced velocity between the installed sharp-edged boulders. For the velocity of seepage flow, the value is kept small. This might be explained as the velocity is limited when the seepage flow goes through the space among small gravels.

At x = 2.32 m, similar velocity fluctuations are observed above the gravel mount as those at x = 1.67 m (Figure 5 (c)). In the region where the cobble stones are installed (0.05 ≦z (m)≦ 0.08), the value of the mean velocity at z = 0.08 m is larger than that in the region of 0.05 ≦z (m)≦0.07. This might be caused by a large difference of mean velocity observed between the water surface flow and the bottom flow near gravel bed. The main flow is located near the water surface, and the water surface flow has a high velocity, whereas the flow near the gravel bed is considerably slower. Furthermore, it should be noted that both Case 1 and Case 2 exhibit similar deviation trend in the time-series data of the velocity for x component.

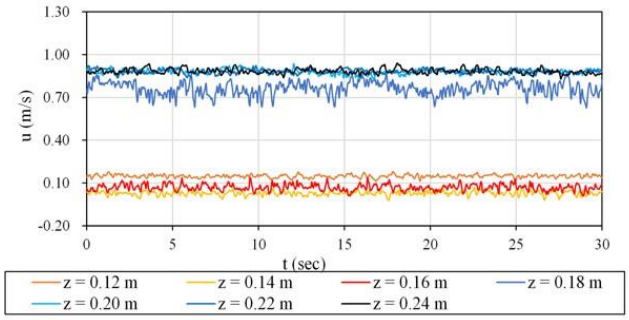

(1) Outer flow region

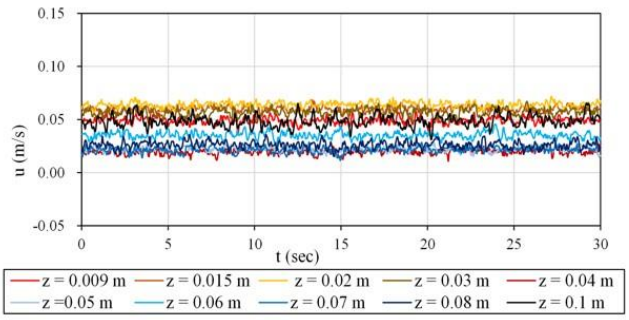

(2) Inner flow region

(a) Time-series of longitudinal velocity at x = 0.75 m

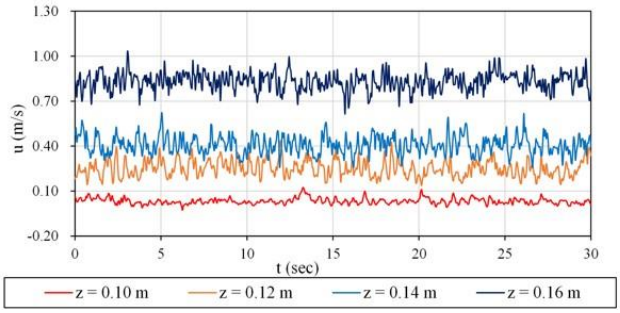

(1) Outer flow region

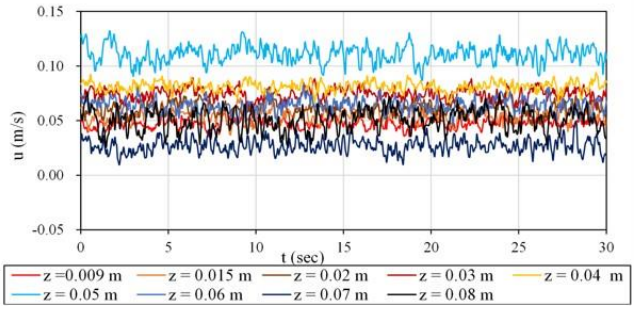

(2) Inner flow region

(b) Time-series of longitudinal velocity at x = 1.67 m

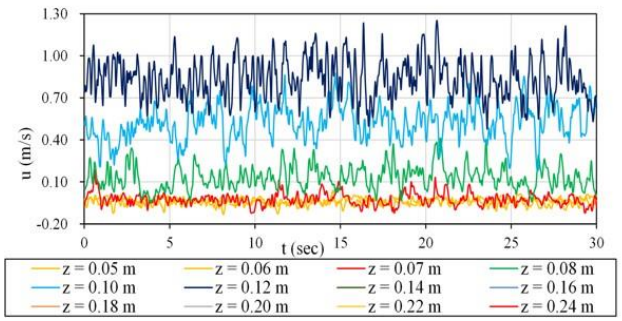

(1) Outer flow region

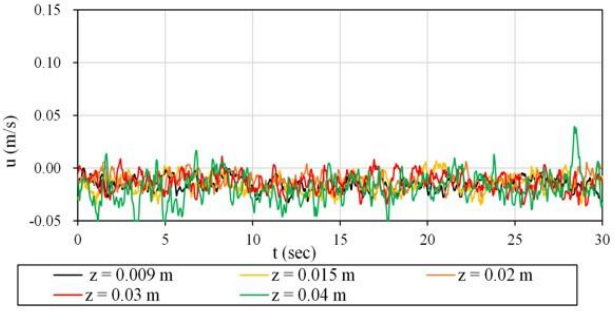

(2) Inner flow region

(c) Time-series of longitudinal velocity at x = 2.32 m

Figure 5. Time-series of longitudinal velocity for Case 2

3.6 Spectral Analysis on the Fluctuating Velocity

Figure 6 shows results of the spectral analysis on the time-series of the longitudinal component of fluctuating velocity for Case 2, for three measurement points: x = 0.75 m, x = 1.67 m, and x = 2.32 m. Spectral analysis assess the intensity of a specific frequency component present in the time-series data presented at paragraph 3.4 . According to the magnitude of the spectrum by period due to the fluctuating velocity in the seepage flow at any position of x, as shown in Figure 6, the larger the frequency, the smaller the spectrum.

In the measurement section of x = 0.75 m, the spectrum at the position of z = 0.18 m is larger than that at other z locations, spanning from low to high frequencies. This might be caused by the intermittent velocity fluctuations that occur close to the upper edge of the boundary layer. At the locations of z = 0.20, 0.22, and 0.24 m, the spectra with periods from 1.0 to 2.0 Hz and from 0.2 to 0.3 Hz are large. This is considered to be the period included in the flow entering the mount. The spectra in the seepage flow do not differ significantly in magnitude from 0.2 to 10 Hz, except at the location of z = 0.10 m.

At the section of x = 1.67 m, the spectra in the region of z ≥ 10 cm are larger than those in the seepage flow, spanning from low to high frequencies. This might be caused by turbulence within the new boundary layer developed from the gravel mount, as indicated by the time series variation. Within the seepage flow, the spectrum is larger regardless of the position of z inside small gravels, compared to that evaluated at x = 0.75 m. This is thought to be due to the increased velocity fluctuations in the upper part of the sedimentary layer.

At the section of x = 2.32 m, the spectrum is larger than that at the section of x = 1.67 m, except for the high frequencies. This might be caused by the effect of a larger velocity gradient just above the sedimentary layer due to the further acceleration of the velocity in the upper part of the sedimentary layer.

In Case 1, the spectra in the upper part of the sedimentary layer are smaller than those in Case 2, but the spectra in the seepage flow are similar to those in Case 2.

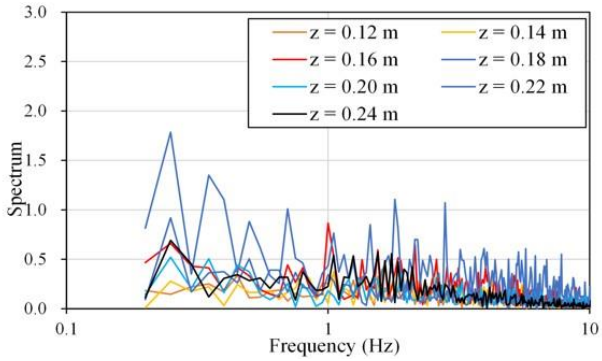

(1) Outer flow region

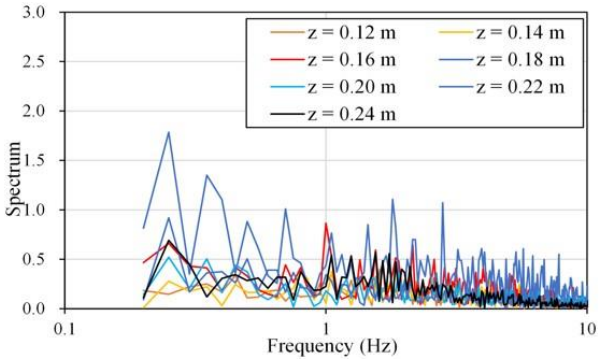

(2) Inner flow region

(a) Spectral analysis on the time-series data corresponding to Figure 5 (a), at x = 0.75 m

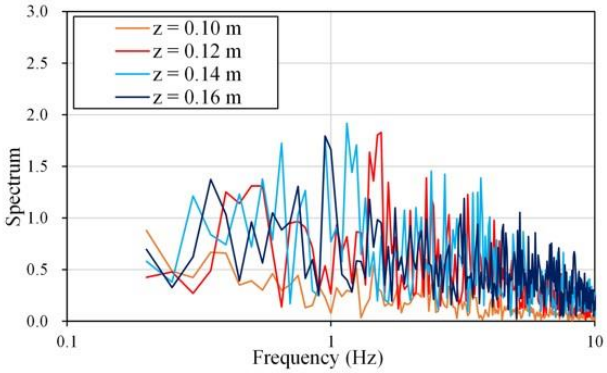

(1) Outer flow region

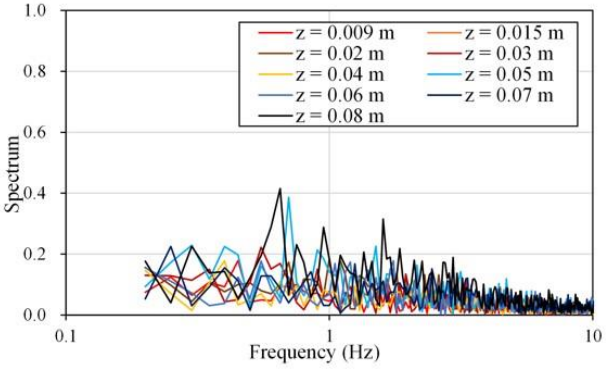

(2) Inner flow region

(b) Spectral analysis on the time-series data corresponding to Figure 5 (b), at x = 1.67 m

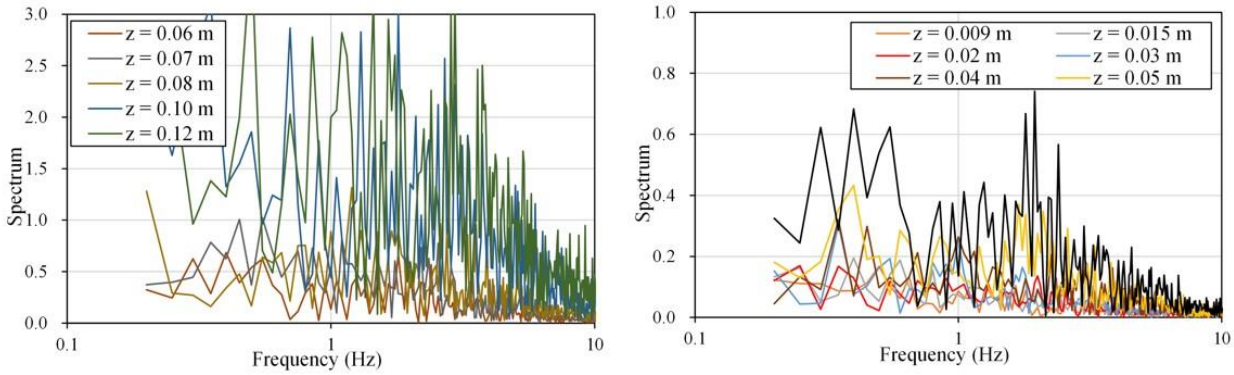

(1) Outer flow region (2) Inner flow region

(c) Spectral analysis on the time-series data corresponding to Figure 5 (c), at x = 2.23 m

Figure 6. Spectral analysis on the time-series data corresponding to Figure 5 (for Case 2)

5. Discussion

The gravel mount with small gravels consisted in a heaped up shape was installed in horizontal rectangular channel in order to form the seepage flow between the small gravels. The water surface gradient is varied by the formation of flow passing through the gravel mount as shown in Figures 1 and 2. The velocity measurement of seepage flow is possible by installing enamel-coated metal coils inside the gravel mount. If the coil is not coated by an enamel liquid, the magnetic field generated by the measuring instrument interferes with the metal of the coil and normal flow velocities cannot be evaluated. According to velocity measurement, small turbulent flows are always formed between small gravels with an average diameter of 0.016 m. In this case, as the seepage flow is not regarded as a laminar flow, the principal based on Darcy law cannot be applied. Mean velocity and turbulent intensity between the small gravels are consistently small in accordance with the velocity measurement due to two-dimensional electrical magnetic current meter. Change of the velocity inside small gravels remains negligibly small in two different discharges. Furthermore, change of the mean velocity $\bar{u}$ with vertical direction is large near the peak of the gravel mount, whereas the turbulent intensity is always small. Spectrum inside the seepage flow revealed that the spectrum is consistently small spanning from low to high frequencies. The flow resistance of the flow over the gravel mount appears to depend on the formation of seepage flow, and turbulence is reduced near the bottom.

6. Conclusion

Gravel mount consisting of gravel with average grain diameter of 0.016 m was installed on the experimental channel to generate seepage flows. Also, the gravel mount was covered with sharp-edged boulders at the upstream section and cobble stones at the downstream section. The experiment was conducted for two different water discharges and mean velocity, standard deviation of flow velocity, time-series of velocity, and result of spectral analysis on velocity fluctuation were examined. Experimental results can be summarized as follows:

a) By installing boulders on top of the gravel mount, the overall structure was stabilized, preventing any gravel from being washed downstream. Therefore, when constructing artificial spawning beds in an actual river, the combination of gravel and boulder is suggested. Additionally, when constructing spawning beds, it is significant that the main flow consistently exists along the water surface both in normal stage and flood stage to prevent the gravels from being washed away.

b) Mean velocity of seepage flow was found to be correlated with water surface slope near the peak of the gravel mount. In this case, the change of mean velocity between the small gravels remained consistently low. Furthermore, the velocity measurements reveal that the velocity of seepage flow does not change for different two discharges except for a change only when there is a difference in the water surface gradient.

c) The time-series variation of the velocity between the small gravels shows that the fluctuation always occurs, although the range of fluctuation is small. Furthermore, the velocity near the gravel bed depends on the water surface gradient of turbulent flow passing over the gravel mount.

d) The spectrum evaluated from the velocity fluctuations inside the gravel mount is always smaller than that

above the gravel mount spanning from low to high frequencies. Turbulence near the gravel bottom is reduced by the formation of seepage flow even if the velocity difference increases in the vertical direction over the gravel mount.

This paper is the result of the first stage of research and shows the results of the study with a limited size of crushed stone. In the future, the size of the crushed stones will be changed to clarify the difference in seepage flow due to the difference in porosity. This will enable artificial regeneration of seepage flow that leads to spawning and temperature control according to the site of the river.

References

Kono, T., Akamatsu, Y., Goto, M., & Inui, R., (2017). Quantification of Plecoglossus altivelis using environmental DNA and trial of monitoring of downstream mitigation. *Advances in River Engineering, 23,* 669-674.

McManamay, A. R., Orth, J. D., Dolloff, A. C., & Cantrell, A. M. (2010). Gravel addition as a habitat restoration technique for tailwaters. *North American Journal of Fisheries Management, 30,* 1238-1257. https://doi.org/10.1577/M10-007.1

Ohtsu, I., & Yasuda, Y. (1994). Characteristics of supercritical flow below sluice gate. *Journal of Hydraulic Engineering, 120*(3), 332-346. https://doi.org/10.1061/(ASCE)0733-9429(1994)120:3(332)

Orchard, E. R. (1988). New method for measuring water seepage through salmon spawning gravel. *United States Department of Agriculture, Forest Service*. https://doi.org/10.2737/PNW-RN-483

Piccoli, B. P., & Yasuda, Y. (2023). Alternated gravel mounts with artificial assembled boulders reinforcement inside channelized rivers. *Journal of Environmental Science Studies, 6*(1), 26-35. https://doi.org/10.20849/jess.v6i1.1352

Schirmer, M., Luster, J., Linde, N., Perona, P., Mitchell, D. A. E., Barry, A. D., … Durisch-Kaiser, E. (2013). Morphological, hydrological, biogeochemical changes and challenges in river restoration – the Thur river case study. *Hydrology and Earth System Sciences Discussions, 18,* 2449-2462. https://doi.org/10.5194/hessd-10-10913-2013

Wheaton, M. J., Pasternack, B. G, & Merz, E. J. (2004). Spawning habitat restoration -I. Conceptual approach and methods. *International Journal of River Basin Management, 2*(1), 3-20. Retrieved from https://www.researchgate.net/publication/37146816

Zhang, H., & Chanson, H. (2015). Free-surface and seepage bubble flows on a gabion stepped spillway weir: experimental observations. *IAHR World Congress.* Retrieved from https://www.iahr.org/library/infor?pid=7754

Copyrights